SUPPLEMENTARY INFORMATION

"Precursor motion to iceberg calving at Jakobshavn Isbræ, Greenland, observed with terrestrial radar interferometry"
By Surui Xie, Timothy H. Dixon, Denis Voytenko, David M. Holland, Denise Holland and Tiantian Zheng

Tidal response of ice speed at Jakobshavn Isbræ

For marine-terminating glaciers like Jakobshavn Isbræ, the influence of ocean tides on ice speed provides opportunities for investigating physical conditions of glacial motion (Gudmundsson, 2011; Podrasky and others, 2014; Walker and others, 2014; Voytenko and others, 2015). Blue and yellow lines in Fig. S3 (b) are the predicted and observed tide rate (i.e., the time derivative of the tide height) at the mouth of Jakobshavn Isbræ's fjord, ∼70 km away from the glacier cliff. Podrasky and others (2014) compared 14 days of tide measurements within 5 km of the calving front and the tides recorded at Ilulissat, and found no measurable delay in time, and a maximum difference in stage of less than 10 cm. Therefore the tide at the mouth of Jakobshavn Isbræ's fjord should closely represent the tidal variations at the glacier cliff. Power spectral density (PSD) estimates of 4 days of velocity time series from Jakobshavn Isbræ show distinct diurnal and semi-diurnal signals. Based on the inference method described by Davis and others (2014), we analyzed tide-induced velocity perturbations. Fig. S3 (a) is the TRI line-of-sight (LOS) velocity map overlain on a Landsat-8 image; S3 (b) shows LOS velocities along an approximate flow line and tide rate time series; S3 (c) shows the phase lag map of M2 ocean tidal constituent (phase lag maps of K1 and S2 show the same pattern). From Fig. S3 (b) and (c) we can see that the phase lag of ocean tide rate increases rapidly between points (4) and (5). This may indicate the location of the grounding line, similar to results of Rosenau and others (2013). In other words, there is a narrow floating zone (∼1 km wide) near the ice cliff.

Analysis of differential stress generated by subsurface melting

Photogrammetry images suggest that the calved block was ∼760 m in its long dimension (T_f, the final thickness of the ice block) (Fig. S4). Assuming the block has a rectangular shape with dimensions of $L \times W \times T$ prior to calving, where L and W are the length (1370 m) and width (290 m), and T is the thickness of the block, then the net vertical force (F) generated by the difference between gravitational and buoyancy forces is:

$$F = \rho_i g T L W - \rho_w g(T - h_a)LW \tag{1}$$

where ρ_i is ice density (917 kg m^{-3}), ρ_w is water density (1000 kg m^{-3}), h_a is the height of ice above the water line (∼90 m), and g is the gravitational acceleration.

Assuming the glacier front was in gravitational-buoyancy equilibrium at the initial state (i.e., $F = 0$), and thickness of ice above the water line was approximately constant before calving, then the initial thickness T is ∼1084 m. If the long dimension of the calved block was 760 m, then it lost ∼30% of its ice due to subsurface melting prior to calving, assuming no other loss (e.g., breakage during calving) or thinning (e.g., flux divergence) mechanisms.

Before calving, the shear stress (τ) on the calving surface caused by melting-induced overweighting can be estimated by :

$$\tau = \frac{F}{L T_c} \tag{2}$$

where T_c is the thickness of the solid ice calving surface, accounting for crevasses, i.e., the vertical dimension of the solid ice calving surface is smaller than T because of surface and basal crevassing. In initial equilibrium state, the shear stress induced by gravity and buoyancy together is 0. At the time of calving, assuming $T_c = T = 760$ m (no crevasses), the shear stress τ is ∼103 kPa. Notice that both the ice block thickness T and T_c are time-variable quantities as subsurface melting is a continuing process and crevasses may grow with time. T could also be larger than the floating block long dimension (T_f) since some parts of the block may have broken off prior to reaching the surface. Table S1 gives estimates of shear stress for different thicknesses of the calved block (T) and the calving surface (T_c).

Laboratory studies suggest that the shear strength of ice is strongly dependent on physical conditions including age, temperature and salinity (Ji and others, 2013; Timco and Weeks, 2010; Timco and Frederking, 1982). Typical shear strengths range from 400 kPa to 1100 kPa, for temperatures in the range −2°C – −20°C. When temperature is higher, shear strength is reduced. Experiments by Timco and Frederking (1982) with ice temperature of −3°C suggest an average shear strength of 500 ± 220 kPa for fresh water ice.

Fig. S5 shows the relation between shear stress and crevasse depth assuming the calved block is 760 m thick, compared to the shear strength estimates of fresh water ice from Timco and Frederking (1982). If ice failure is caused by the shear stress generated by subsurface melting and resulting loss of buoyancy, it is either because the crevasses on the calving plane are very deep (>60 % of block thickness), or the effective shear strength of the calving block is much smaller than the laboratory result. Images from both TRI and Landsat-8 show that the calving front in Jakobshavn Isbræ is heavily crevassed, but these images do not allow an estimate of the depth extent of crevassing. Our TRI-derived ice velocity and phase lags relative to ocean tides suggest a ∼1 km wide floating zone at the calving front (Fig. S3). At 34 m d^{-1} (estimated by feature tracking, see main paper), ice in this floating zone will experience ∼29 days of tidal flexing after initial floatation and flexing, which could extend the depth of crevasses. Modeling of ice velocity in the terminal zone of Helheim Glacier in southeast Greenland has suggested that the effective strength of ice in the terminal zone is significantly less than laboratory-derived values (Voytenko and others, 2015).

Block rotation rate and tidal forcing

The blue line in Fig. S6 shows tidal variations at the mouth of Jakobshavn Isbræ's fjord. The calving event happened at low tide. The Pearson's correlation coefficient between rotation rate (subtracting the ice failure curve) and tide is -0.07, while tide rate gives -0.01, suggesting no linear correlation between block rotation rate and tide or tide rate.

REFERENCES

Davis JL, De Juan J, Nettles M, Elosegui P, Andersen ML (2014) Evidence for non-tidal diurnal velocity variations of Helheim Glacier, East Greenland. *J. Glaciol.*, **60**(224), 1169–1180 (doi: 10.3189/2014JoG13J230)

Gudmundsson GH (2011) Ice-stream response to ocean tides and the form of the basal sliding law. *The Cryosphere*, **5**(1), 259–270 (doi: 10.5194/tc-5-259-2011)

Ji SY, Liu HL, Li PF, Su J (2013) Experimental Studies on the Bohai Sea Ice Shear Strength. *Journal of Cold Regions Engineering*, **27**(4), 244–254 (doi: 10.1061/(ASCE)CR.1943-5495.0000060)

Podrasky D, Truffer M, Lüthi M, Fahnestock M (2014) Quantifying velocity response to ocean tides and calving near the terminus of Jakobshavn Isbræ, Greenland. *J. Glaciol.*, **60**(222), 609–621 (doi: 10.3189/2014JoG13J130)

Richter A, Rysgaard S, Dietrich R, Mortensen J, Petersen D (2011) Coastal tides in West Greenland derived from tide gauge records. *Ocean Dynamics*, **61**(1), 39–49 (doi: 10.1007/s10236-010-0341-z)

Rosenau R, Schwalbe E, Maas HG, Baessler M and Dietrich R (2013) Grounding line migration and high-resolution calving dynamics of Jakobshavn Isbræ, West Greenland. *J. Geophys. Res.-Earth Surf.*, **118**(2), 382–395 (doi: 10.1029/2012JF002515)

Timco GW and Weeks WF (2010) A review of the engineering properties of sea ice. *Cold Regions Science and Technology*, **60**(2), 107–129 (doi: 10.1016/j.coldregions.2009.10.003)

Timco GW and Frederking RM (1982) Comparative strengths of fresh water ice. *Cold Regions Science and Technology*, **6**(1), 21–27 (doi: 10.1016/0165-232X(82)90041-6)

Voytenko D, Stern A, Holland DM, Dixon TH, Christianson K and Walker RT (2015) Tidally-driven ice speed variation at Helheim Glacier, Greenland observed with Terrestrial Radar Interferometry. *J. Glaciol.*, **61**(226), 301–308 (doi: 10.3189/2015JoG14J173)

Walker RT, Parizek BR, Alley RB, Brunt KM, Anandakrishnan S (2014) Ice-shelf flexure and tidal forcing of Bindschadler Ice Stream, West Antarctica. *Earth and Planetary Science Letters*, **395**, 184–193 (doi: 10.1016/j.epsl.2014.03.049)

Table S1. Shear stress (kPa) generated by the calved block as a function of thickness, T. Percentage numbers in the first column indicate the amounts of subsurface melting compared to the ice block in the initial equilibrium state. Shear stress increases with decrease of calving surface thickness (T_c).

T	T_c									
(m)	$1.0T$	$0.9T$	$0.8T$	$0.7T$	$0.6T$	$0.5T$	$0.4T$	$0.3T$	$0.2T$	$0.1T$
760 (30%)	103	114	128	147	171	205	257	342	514	1027
800 (26%)	86	95	107	122	143	171	214	285	428	856
850 (22%)	66	74	83	95	111	133	166	221	332	664
900 (17%)	49	55	62	70	82	99	123	164	247	493
950 (12%)	34	38	43	49	57	68	85	113	170	340

$$D = 25.0 + 0.6t + 0.0043t^2 - 9.1H(t + 28.5)$$
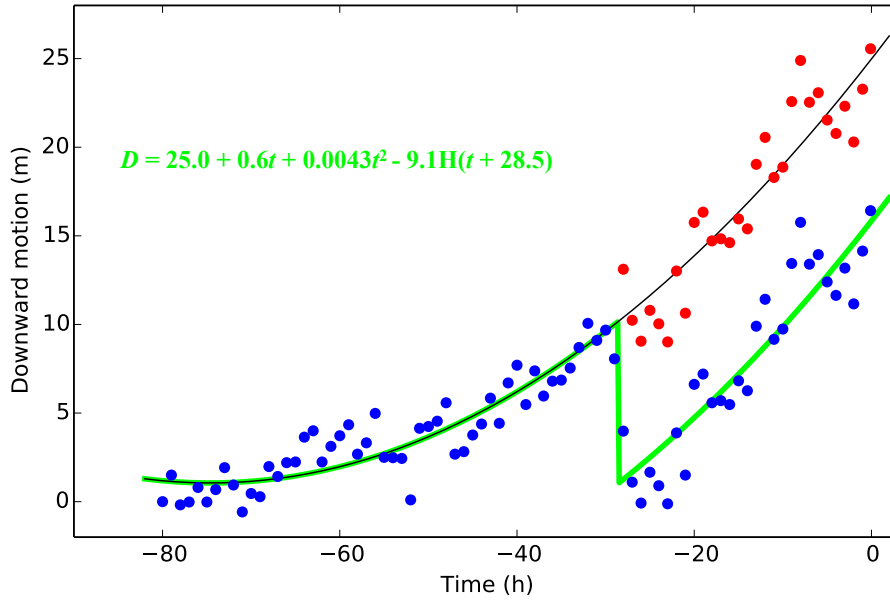
Fig. S1. Ice block downward motion versus time (compare to Fig. 8 in the main paper, rotation rate versus time). Blue dots are vertical displacement estimates; red dots are downward motion corrected by adding a Heaviside (H) step function after an ice failure event $\sim$28.5 hours before the main calving event (equation, upper left). Green and black curves are the best fits of downward displacement time series before and after correction, assuming simple parabolic behavior.
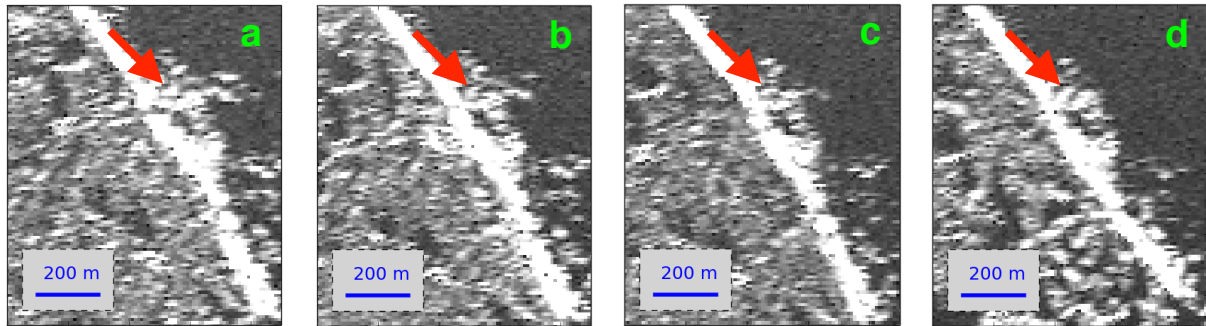
Fig. S2. TRI intensity images of the calving block on four successive days. All images have the same scale and are in the same fixed Cartesian system. The glacier front is indicated by red arrow, observable ice surface becomes narrower as the up-glacier side subsides and is shadowed by the higher down-glacier side. (a) 2015-06-07 00:01:00 UTC. (b) 2015-06-08 00:01:00 UTC. (c) 2015-06-09 00:01:00 UTC. (d) 2015-06-10 00:01:00 UTC.
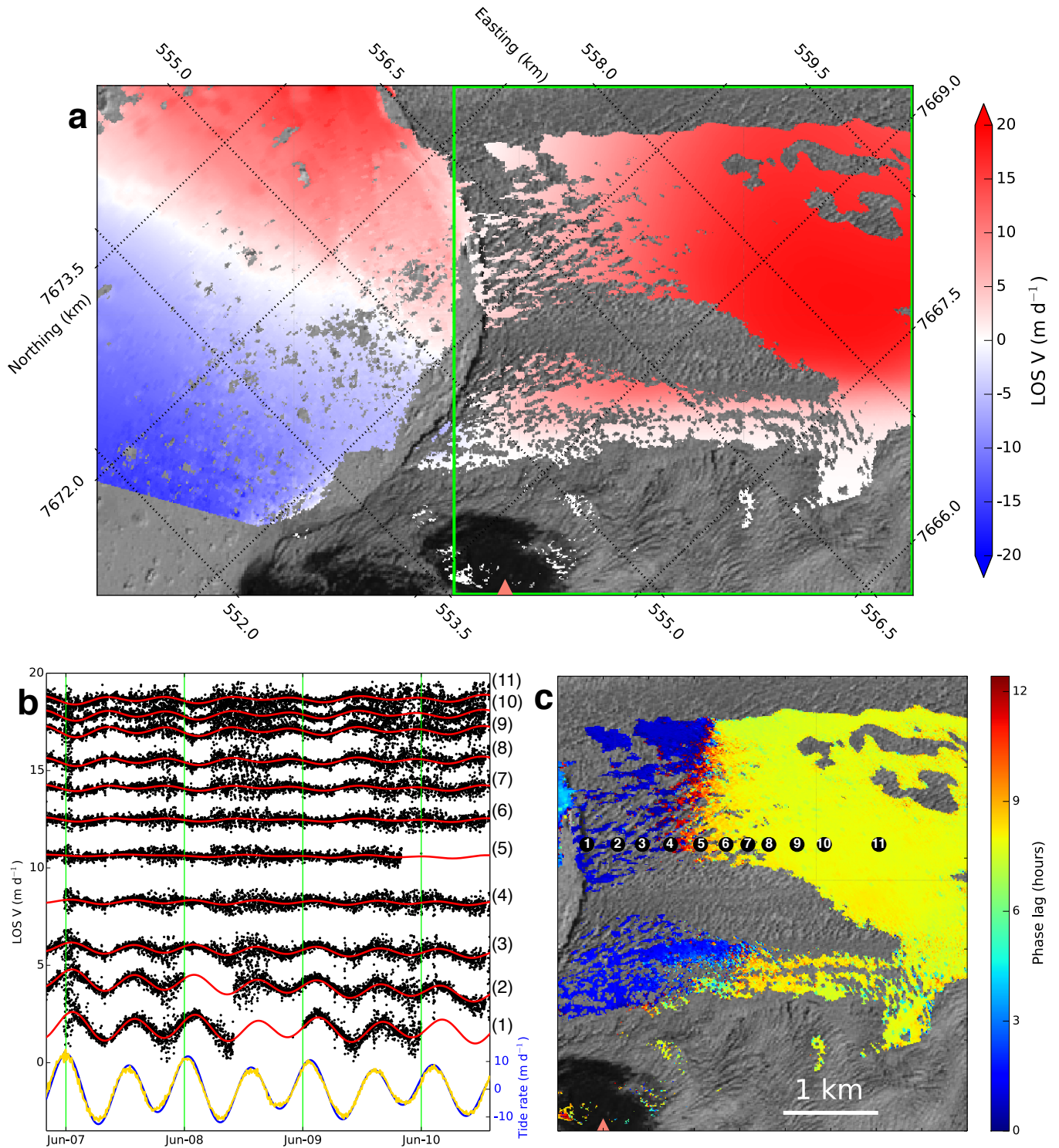
Fig. S3. Ice velocity and tidal response. (a) Averaged LOS velocity map of the glacier terminus from 4 days of TRI measurements. Velocity is positive when ice moves towards the radar (salmon triangle). Green box outlines the area of phase lag map in (c). (b) LOS velocity from TRI (black) and tide rate (blue/yellow) time series. (1) - (11) indicate location of points in (c). Red curves are model fits to LOS velocities, considering linear velocities and three periodic signals with the frequencies of K1/M2/S2 tidal constituents, from Richter and others (2011). Blue line is the predicted tide rate, yellow line is the tide rate derived from measured tide height time series (10 minute sampling rate) from the mooring at the mouth of the fjord at Jakobshavn Glacier. (c) Phase lags for the largest tidal constituent (M2) overlain on a Landsat-8 image. One colour cycle corresponds to one period, so the phase of red is close to the phase of blue. Only points with longer than 2 days observation and more than 50% of acquisitions are analyzed. Notice the phase lags increase rapidly between (4) and (5). There is a ~1 km wide zone near the terminus that has very small phase lag. The estimates near shore are noisy because of nearly stagnant ice, with rates similar to the uncertainty of TRI measurements.

Fig. S4. Image of the calved block. Most of the block remains intact immediately after the calving event. The long dimension is about 760 meters.
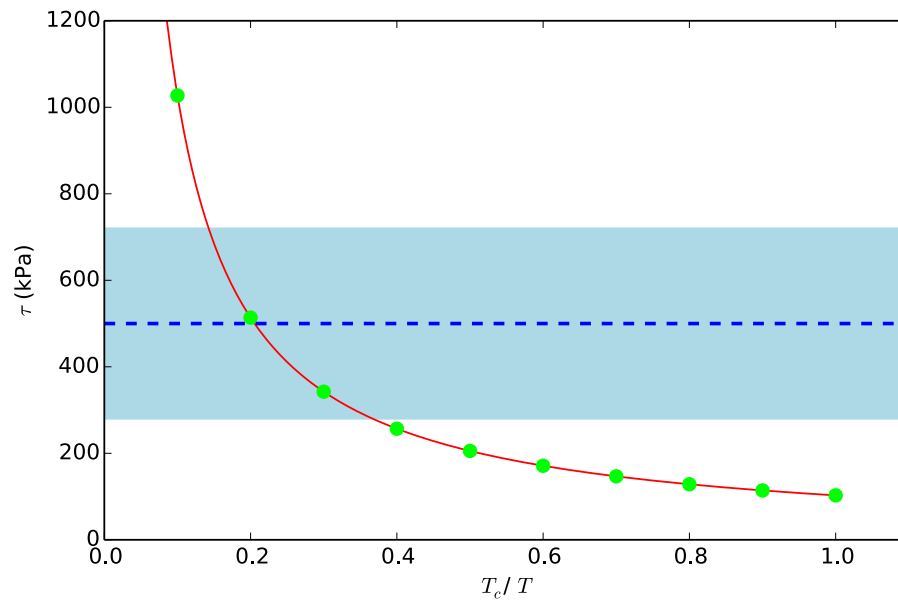
Fig. S5. Shear stress (τ) versus ratio of thickness on the calving surface (T_c) to thickness of the ice block (T), when $T = 760$ m. Green dots represent shear stress when T_c/T varies from 0.1, 0.2, ..., 1.0. Red curve is the inverse function of shear stress against T_c/T. Blue dashed line and light blue area ($\tau = 500 \pm 220$ kPa) mark the shear strength of fresh water ice from Timco and Frederking (1982).
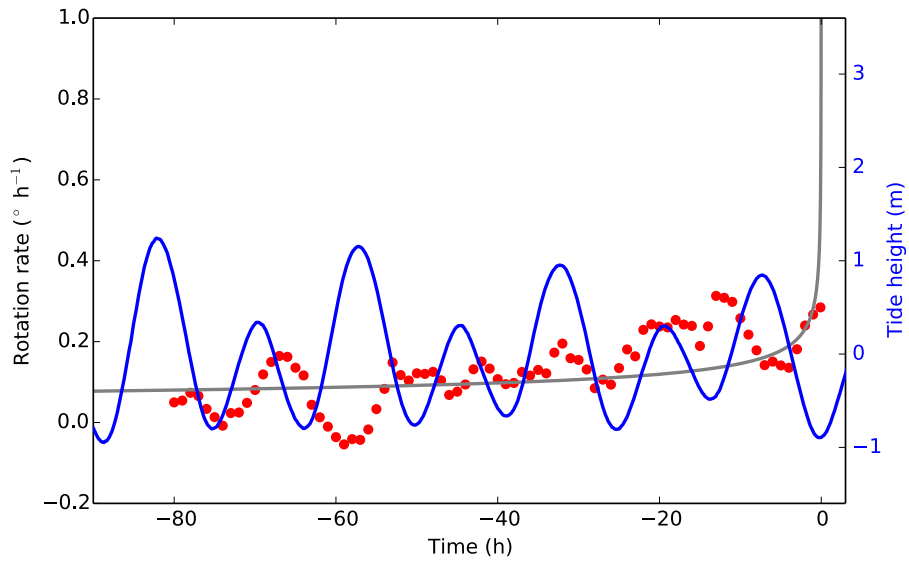
Fig. S6. Block rotation rate (red) and tide height (blue). Grey curve is the best fit of ice failure model, setting the rotation rate to infinity at the known time of the calving event ($t = 0$). The Pearson's correlation coefficient between rotation rate (subtracting the grey curve) and tide is -0.07, while with tide rate it is -0.01, suggesting no linear correlation between block rotation rate and tide or tide rate.